Cement & Concrete Composites 34 (2012) 342–348

Contents lists available at SciVerse ScienceDirect

Cement & Concrete Composites

journal homepage: www.elsevier.com/locate/cemconcomp

Improved fiber distribution and mechanical properties of engineered cementitious composites by adjusting the mixing sequence

Jian Zhou [a,*], Shunzhi Qian [b], Guang Ye [c,d], Oguzhan Copuroglu [c], Klaas van Breugel [c], Victor C. Li [e]

[a] Sinoma Research Institute, Sinoma International Engineering Co., Ltd., Beijing, China
[b] School of Transportation, Southeast University, Nanjing, China
[c] Microlab, Faculty of Civil Engineering and Geosciences, Delft University of Technology, Delft, The Netherlands
[d] Magnel Laboratory for Concrete Research, Department of Structural Engineering, Ghent University, Technologiepark-Zwijnaarde 904, B-9052 Ghent (Zwijnaarde), Belgium
[e] Department of Civil and Environmental Engineering, University of Michigan, USA

ARTICLE INFO

Article history:
Received 12 November 2010
Received in revised form 26 November 2011
Accepted 28 November 2011
Available online 6 December 2011

Keywords:
Engineered cementitious composites
Mixing sequence
Fiber distribution
Tensile strain capacity
High volume of sand

ABSTRACT

Engineered cementitious composites (ECC) is a class of ultra ductile fiber reinforced cementitious composites, characterized by high ductility and tight crack width control. The polyvinyl alcohol (PVA) fiber with a diameter of 39 μm and a length of 6–12 mm is often used. Unlike plain concrete and normal fiber reinforced concrete, ECC shows a strain-hardening behavior under tensile load. Apart from the mix design, the fiber distribution is another crucial factor for the mechanical properties of ECC, especially the ductility. In order to obtain a good fiber distribution, the plastic viscosity of the ECC mortar before adding fibers needs to be controlled, for example, by adjusting water-to-powder ratio or chemical admixtures. However, such adjustments have some limitations and may result in poor mechanical properties of ECC. This research explores an innovative approach to improve the fiber distribution by adjusting the mixing sequence. With the standard mixing sequence, fibers are added after all solid and liquid materials are mixed. The undesirable plastic viscosity before the fiber addition may cause poor fiber distribution and results in poor hardened properties. With the adjusted mixing sequence, the mix of solid materials with the liquid material is divided into two steps and the addition of fibers is between the two steps. In this paper, the influence of different water mixing sequences is investigated by comparing the experimental results of the uniaxial tensile test and the fiber distribution analysis. Compared with the standard mixing sequence, the adjusted mixing sequence increases the tensile strain capacity and ultimate tensile strength of ECC and improves the fiber distribution. This concept is further applied in the development of ECC with high volume of sand.

1. Introduction

ECC, short for engineered cementitious composites, is a class of ultra ductile fiber reinforced cementitious composites invented in the early 1990s [1]. The polyvinyl alcohol (PVA) fiber with a diameter of 39 μm and a length of 6–12 mm is often used. This group of materials is characterized by high ductility and tight crack width. Fig. 1 shows a typical tensile stress–strain curve of ECC and its tight crack width control [2]. Unlike plain concrete and normal fiber reinforced concrete, ECC shows a tensile strain-hardening behavior after first cracking and develops a high tensile ductility in the range of 3–7%. The crack width of ECC is self-controlled to around 60 μm without the presence of steel reinforcement, which is much smaller than the typical crack width observed in the steel reinforced concrete. ECC thus shows lower water permeability [3] and better durability [4–6] compared with standard concrete. The use of ECC can prolong the service life of structures and reduce the maintenance and repair cost. Nowadays ECC is emerging in broad applications, such as ECC link slab on bridge decks [7], ECC coupling beam in high-rise buildings to enhance their seismic resistance, composite ECC/steel bridge deck and some concrete repair applications [8].

This unique tensile strain-hardening behavior results from an elaborate ECC design methodology, which uses a micromechanics model. This micromechanics model takes into account the interactions among fiber, matrix and fiber–matrix interface [9]. Apart from the mix design, the fiber distribution is another crucial factor for the mechanical properties of ECC, especially the ductility. Torigoe et al. [10] found a strong correlation between the fiber distribution and the tensile strain capacity of ECC. A poor fiber distribution leads to a decrease in ductility and even absence of the strain-hardening behavior. In order to improve the fiber distribution, a high plastic viscosity of the fresh ECC mortar before the fiber addition is desirable [11]. For an adequate plastic viscosity, the

* Corresponding author.
E-mail address: ZhouJian@sinoma.com.cn (J. Zhou).

0958-9465/$ - see front matter © 2011 Elsevier Ltd. All rights reserved.
doi:10.1016/j.cemconcomp.2011.11.019

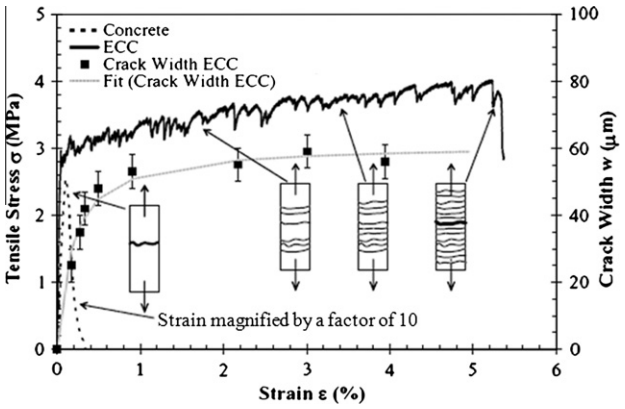

Fig. 1. Tensile stress–strain curve and tight crack width control of ECC [2].

water-to-powder (w/p) ratio of ECC mortar before mixing fibers needs to be controlled. However, the low w/p ratio could cause the increase in the yield stress of the fresh ECC and thus the loss of workability. Moreover, the low w/p ratio results in a strong ECC matrix, causing a decrease in ductility [11]. The ECC mix design is, therefore, limited in a small range of w/p ratio, mainly from 0.2 to 0.3 [11]. This is similar for solid materials. For instance, since the addition of aggregates can cause balling of fibers at mixing and poor fiber distribution [12].

This research explores an innovative approach, focusing on adjusting the ECC mixing sequence to improve the fiber distribution. As shown in Fig. 2, the standard mixing sequence is carried out as follows: (1) all solid and liquid materials are first mixed for several minutes; (2) fibers are added and mixed. The plastic viscosity of ECC mortar before the fiber addition determines the fiber distribution in matrix. Consequently, if the fresh properties do not reach the condition for a good fiber distribution, although the mix design is appropriate, ECC will not show good hardened properties [11]. With the adjusted mixing sequence, the mix of solid materials with the liquid material is divided into two steps and the addition of fibers is between the two steps. As shown in Fig. 3, proper amounts of powder and liquid materials are first mixed, aiming at a desirable plastic viscosity for the good fiber distribution [11]. Then, fibers are added. After fibers are mixed homogenously, the rest powder and/or liquid materials are added to tailor the workability and the hardened properties of ECC. As a result, the fiber distribution is improved and ECC shows robust fresh and hardened properties.

This paper aims to investigate the improved fiber distribution by adjusting the mixing sequence. Yang et al. [11] have reported that w/p ratio has a significant effect on the fiber distribution in ECC. Therefore, the different water mixing sequences are first

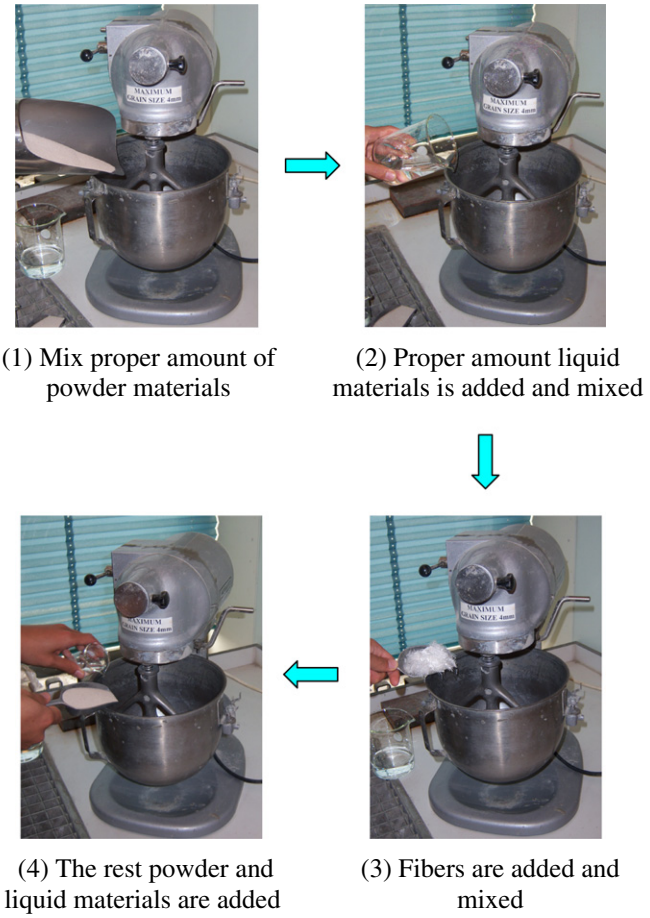

Fig. 3. Adjusted ECC mixing sequence.

studied as an example to demonstrate the advantages of the adjusted mixing sequence. The influence of different mixing sequences is investigated by comparing the experimental results of uniaxial tensile test and fiber distribution analysis. Then, the application of the adjusted mixing sequence in the development of high-volume sand ECC (HVS-ECC) is presented.

2. Experimental program

2.1. Materials

The mix compositions of ECC are given in Table 1. All mixtures had the same mix composition of solid materials and the different

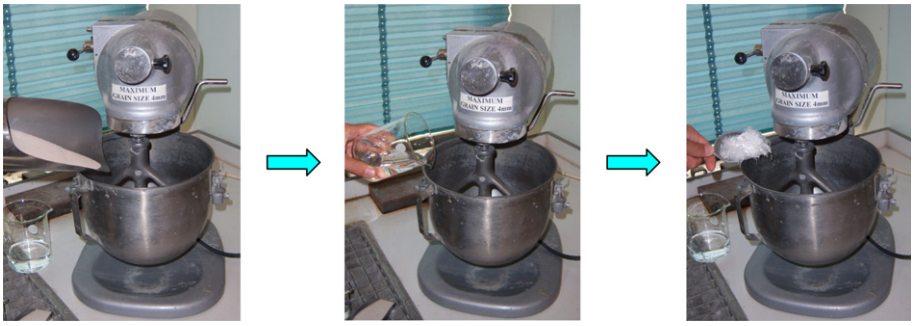

Fig. 2. Standard ECC mixing sequence.

Table 1
Mix compositions of ECC.

Mixture	LP[#]/PC[*]	BFS/PC	w/p ratio	PC (kg/m^3)	LP (kg/m^3)	BFS (kg/m^3)	Water (kg/m^3)	SP[$] (kg/m^3)	PVA fiber (kg/m^3)
M1&M1A	2	1.2	0.3	356	711	427	448	7.1	26
M2&M2A	2	1.2	0.35	330	661	397	486	6.6	26

[#] LP represents limestone powder.
[*] PC represents Portland cement CEM I 42.5N.
[$] SP represents superplasticizer.

Table 2
Chemical compositions of CEM I 42.5N, limestone powder and BFS (by mass). The data of CEM I 42.5N and limestone powder were from the producer and that of BFS was measured by energy dispersive X-ray analysis.

Compound	CEM I 42.5N (%)	Limestone powder (%)	BFS (%)
CaO	64.1	–	40.77
SiO_2	20.1	0.26	35.44
Al_2O_3	4.8	0.08	12.98
Fe_2O_3	3.2	0.06	0.53
MgO	–	0.21	7.99
K_2O	0.52	–	0.49
Na_2O	0.28	–	0.21
SO_3	2.7	–	0.1
$CaCO_3$	–	98.8	–

w/p ratios. M1 and M1A had a w/p ratio of 0.3, and M2 and M2A had a w/p ratio of 0.35. M1 and M2 were mixed following the standard mixing sequence, while M1A and M2A were mixed following the adjusted mixing sequence. The mixing sequence is described in detail in Section 2.2.

Table 2 lists the chemical compositions of CEM I 42.5N, limestone powder and blast furnace slag (BFS). The densities of CEM I 42.5N, limestone powder and BFS were 3150 kg/m^3, 2700 kg/m^3 and 2850 kg/m^3, respectively. The Blaine values of CEM I 42.5N, limestone powder and BFS were 310 m^2/kg, 480 m^2/kg and 320 m^2/kg, respectively. In all mixtures, the fiber content was 2% by volume. Fiber used in this study was the PVA fiber with a length of 8 mm and a diameter of 39 μm, and the fiber aspect ratio was 205. The tensile strength of the PVA fiber is 1600 MPa and the density is 1300 kg/m^3. The surface of the fiber is coated with 1.2% oil by weight to optimize the properties of the fiber–matrix interface, aiming at achieving the strain-hardening behavior and high ductility [13].

2.2. Mixing

M1 and M2 were mixed following the standard mixing sequence as follows:

(1) All water were mixed with solid materials and superplasticizer at low speed for 1 min and then at high speed for 2 min.
(2) PVA fibers were added and mixed at high speed for 4 min.

M1A and M2A were mixed following the adjusted mixing sequence with two-step water addition as follows:

(1) Part of water, with the w/p ratio of 0.27 in the reasonable range [11], was mixed with solid materials and superplasticizer at low speed for 1 min and then at high speed for 2 min.
(2) PVA fibers were added and mixed at high speed for 2 min.
(3) The rest water was added and mixed at high speed for another 2 min.

In total, the standard and adjusted mixing sequences hold the same mixing time of 7 min.

2.3. Casting and curing

The fresh ECC was cast into coupon specimens with the dimension of 240 mm × 60 mm × 10 mm. The specimens were covered with plastic paper and cured for 1 day at a temperature of 20 °C. Then, the specimens were demoulded and cured under sealed condition at a temperature of 20 °C for another 27 days.

2.4. Uniaxial tensile test

The uniaxial tensile test was conducted on the coupon specimens at the age of 28 days as shown in Fig. 4. Four measurements were done for each mixture. Before testing, coupon specimens were sanded for a flat surface and four aluminum plates were then glued on two ends of each specimen. After 1-day curing of the glue, the specimen was fixed on the test set-up by clamping the aluminum plate-glued ends with two pairs of steel plates, which were connected to the loading device. Then, two LVDTs were attached on both sides of the specimen to measure the specimen deformation. The tests were conducted with displacement control at a loading rate of 0.005 mm/s. The testing gauge length was 70 mm. The testing procedure was described in detail in [14].

2.5. Fiber distribution analysis

After the uniaxial tensile tests, four thin sections, perpendicular to the loading direction, were taken from each specimen. The dimension of the thin sections was 30 × 10 mm^2. The samples were glued on a glass and ground. The ground surface was glued to an objective glass. They were sawn to a thickness of around 1 mm. Then, the sawn surface was ground until the thickness of the thin section reached 100 μm.

Images were captured with a magnification of 100× from the samples by optical microscope with plane polarization mode. Sixty images were taken from all of the four pieces from each specimen. In the images, the fibers appear white and the matrix appears black as shown in Fig. 5 left. Then, the images were converted into binary images to segment the fibers. In the binary images as shown in Fig. 5 right, black dots indicate the fibers and the rest indicates the matrix. The number of the fibers in the binary images was counted digitally. With the variation coefficient of the number of the fibers in sixty images, the fiber distribution coefficient was calculated as follows [15]:

$$\alpha = \exp\left(-\sqrt{\frac{\sum(X_i/X_{\text{average}}-1)^2}{n}}\right) \quad (1)$$

where X_i is the number of the fibers in the ith image, X_{average} is the average number of the fibers in all images, and n is the number of images.

3. Results and discussion

3.1. Uniaxial tensile test

The uniaxial tensile stress–strain curves of all mixtures at the age of 28 days are plotted in Fig. 6. Under the uniaxial tensile load-

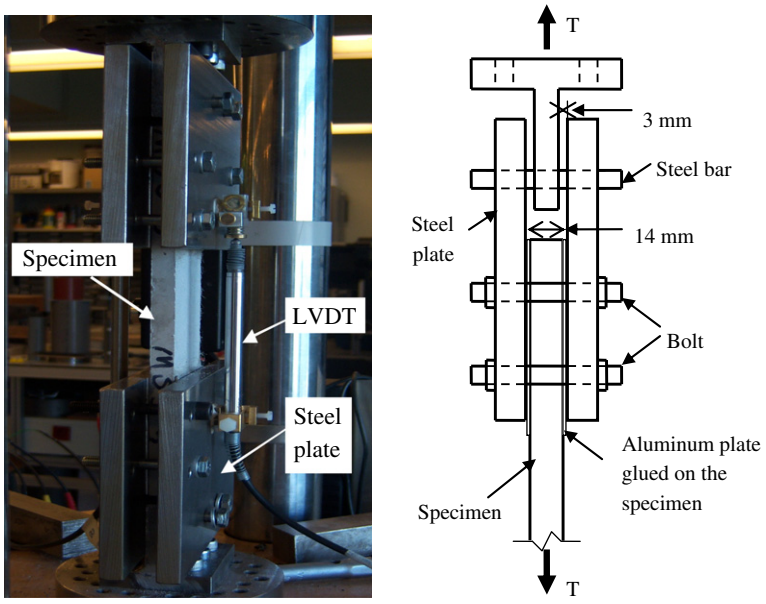

Fig. 4. Uniaxial tensile test set-up.

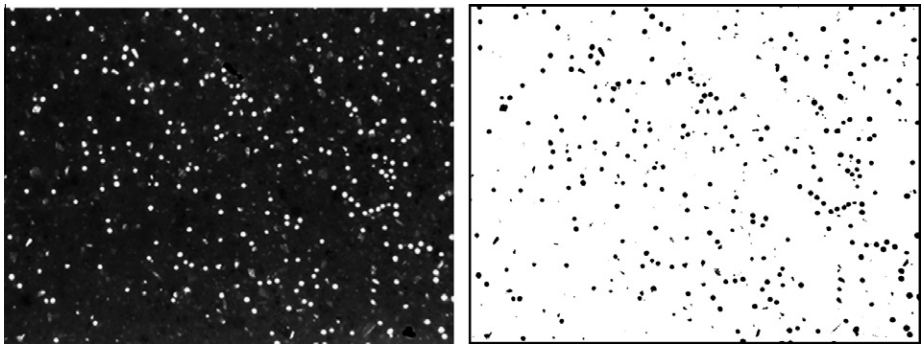

Fig. 5. Image captured on the thin section (left) and corresponding binary image (right).

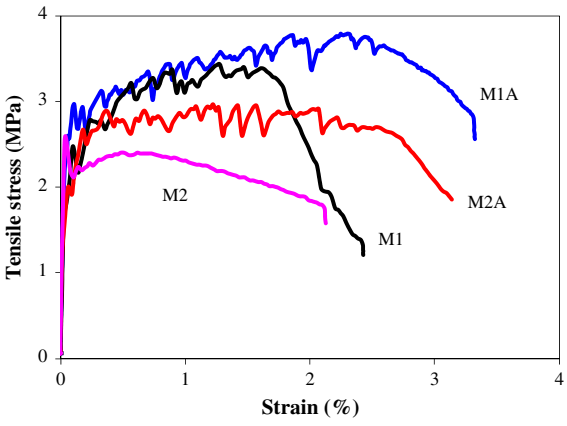

Fig. 6. Typical uniaxial tensile stress–strain curves of the four mixtures at the age of 28 days. M1 and M2 were mixed following the standard mixing sequence, and M1A and M2A were mixed following the adjusted mixing sequence.

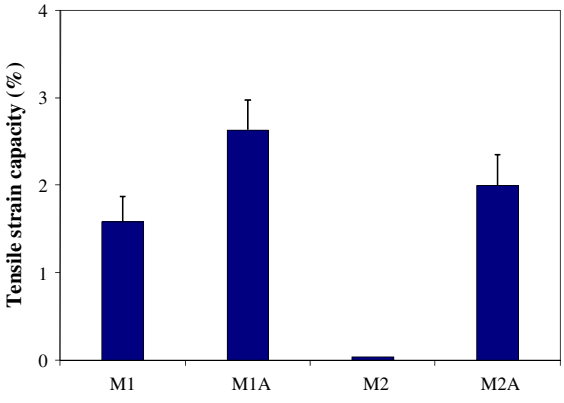

Fig. 7. Tensile strain capacity of the four mixtures at the age of 28 days. M1 and M2 were mixed following the standard mixing sequence, and M1A and M2A were mixed following the adjusted mixing sequence.

ing, M2 shows a single-cracking behavior, while the other mixtures all show a multiple-cracking behavior. The uniaxial tensile stress–strain curve of M2 is featured by a prominent peak at very little strain corresponding to the only cracking. For the mixtures M1, M1A and M2A, the tensile stress increases dramatically at the very beginning and then drops. The first stress drop corresponds to the first cracking in the specimen. The peak stress is called the first cracking strength, which is related to the tensile strength of the matrix. Subsequently, as the tensile stress increases slowly, the specimens exhibit strain-hardening and multiple-cracking behavior.

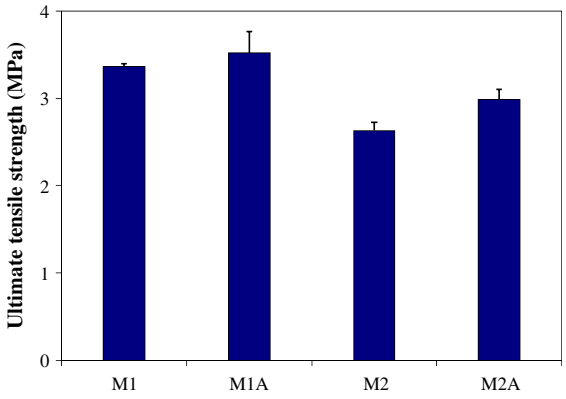

Fig. 8. Ultimate tensile strength of the four mixtures at the age of 28 days. M1 and M2 were mixed following the standard mixing sequence, and M1A and M2A were mixed following the adjusted mixing sequence.

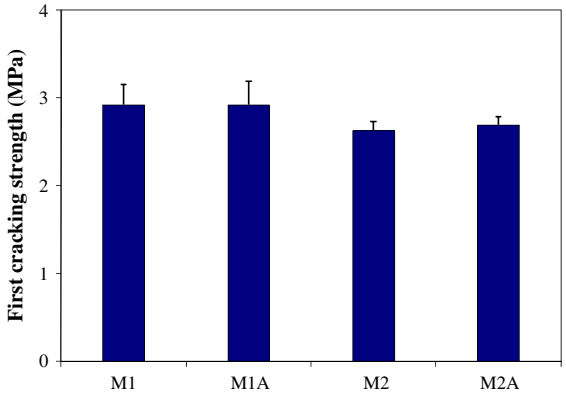

Fig. 9. First cracking strength of the four mixtures at the age of 28 days. M1 and M2 were mixed following the standard mixing sequence, and M1A and M2A were mixed following the adjusted mixing sequence.

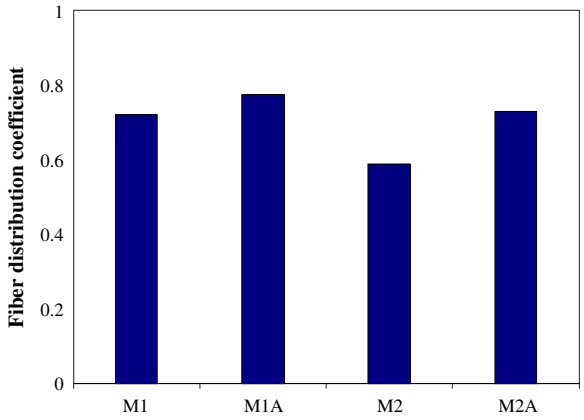

Fig. 10. Fiber distribution coefficient of the four mixtures. M1 and M2 were mixed following the standard mixing sequence, and M1A and M2A were mixed following the adjusted mixing sequence.

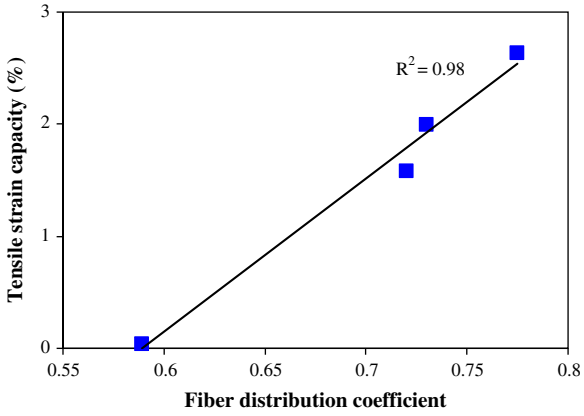

Fig. 11. Correlation between the fiber distribution coefficient and the tensile strain capacity.

Figs. 7–9 show the tensile strain capacity, the ultimate tensile strength and the first cracking strength of the four mixtures, calculated by averaging the results of the four measurements for each mixture. The ultimate tensile strength is defined as the maximum stress in the tensile stress–strain curve, and the corresponding strain is called the tensile strain capacity. As the w/p ratio increases, for both the mixtures mixed following the standard mixing sequence and those with the adjusted mixing sequence, the tensile strain capacity and the ultimate tensile strength decrease. For the same w/p ratio, the mixtures mixed following the adjusted mixing sequence (M1A and M2A) show a greater strain capacity and a higher ultimate tensile strength than the mixtures mixed following the standard mixing sequence (M1 and M2), respectively. The increases in the strain capacity and of the ultimate tensile strength appear more prominent in the mixtures with a higher w/p ratio. The mixtures with the w/p ratio of 0.3 show a 66% increase in the tensile strain capacity and a 5% increase in the ultimate tensile strength. For the mixtures with the w/p ratio of 0.35, M2A retains a tensile strain capacity of 2%, which is more than 50 times that of M2. The ultimate tensile strength of M2A is 14% higher than that of M2. As shown in Fig. 9, M1A and M2A have a slightly higher first cracking strength than M1 and M2, respectively. The first cracking strength mainly relates to the tensile strength of ECC matrix. It means that the different mixing sequences do not have significant effect on the properties of the ECC matrix.

3.2. Fiber distribution coefficient

A higher fiber distribution coefficient indicates a more uniform fiber distribution. The maximum value of the fiber distribution coefficient is 1, which means that the number of the fibers in every image is the same. Fig. 10 shows the fiber distribution coefficient. The fiber distribution coefficient of M1A is 8% higher than that of M1, and the distribution coefficient of M2A is 24% higher than that of M2. The increased fiber distribution coefficients indicate that adjusting the mixing sequence indeed improves the fiber distribution in ECC. Besides, the improved fiber distribution is also confirmed by the observation of many fiber bundles in the mixing with the standard sequence rather than with the adjusted sequence.

The correlation between the tensile strain capacity and the fiber distribution coefficient is plotted in Fig. 11. The tensile strain capacity shows a strong correlation with the fiber distribution coefficient. The experimental results imply that a more uniform fiber distribution is desirable for higher tensile ductility. The improved fiber distribution explains the better tensile properties of the mixtures mixed following the adjusted mixing sequence.

4. Discussion

The PVA fibers are provided in the form of fiber bundles. In order to separate the fiber bundles and to mix fibers uniformly, high

Table 3
Mix compositions of ECC and HVS-ECC (kg/m^3).

Mixture	CEM I 42.5N	Limestone powder	BFS	Silica fume	River sand	Water	W/p ratio	Super-plasticizer	PVA fiber
S1	235	782	547	78	0	410	0.25	15.6	26
S2&S2A	145	482	337	48	1012	253	0.25	9.6	16.1

plastic viscosity of fresh mortar before fiber addition is desirable [11]. The adequate plastic viscosity can be achieved by properly adjusting the w/p ratio and the dosage of superplasticizer. A reasonable w/p ratio should be in the range of 0.25 ± 0.05 for the standard mixing sequence [11]. Beyond this range, the inappropriate fresh properties may lead to non-uniform fiber distribution and thus decrease in hardened properties. The poor tensile properties and poor fiber distribution of M2 with the w/p ratio of 0.35 support this conclusion.

The experimental results in this study reveals that the adjusted mixing sequence can improve the fiber distribution. For the adjusted mixing sequence, a proper amount of water, instead of all, are mixed with the solid materials and superplasticizer aiming at required rheological properties. When fibers are added, the adequate plastic viscosity leads to uniform fiber distribution. Then, the addition of the rest water does not cause significant effect on the fiber distribution. Although the final w/p ratio exceeds the desirable value, a good fiber distribution in ECC can be achieved by properly adjusting the mixing sequence. As shown in the experimental results, although M2A has the same mix composition as M2, M2A, mixed following the adjusted sequence, shows a much more uniform fiber distribution and better hardened properties than M2, mixed following the standard sequence.

Extending this concept, the fiber distribution is possible to be improved by adjusting the mixing sequence of the other ingredients, such as solid materials and chemical admixtures. ECC is first mixed with a certain mix composition having good fiber distribution. After fibers are mix homogenously, the rheological and mechanical properties of fresh and hardened ECC are tailored by adjusting water, solid materials and/or chemical admixtures according to the requirement of rheological properties and the ECC design theory. This concept resulted in the development of ECC mixtures with the good fresh and hardened properties, such as high volume sand ECC (HVS-ECC) [16].

5. Applications of the concept of adjusting the mixing sequence in the development of HVS-ECC

With the presence of fibers, the addition of aggregates can cause balling at mixing and poor fiber distribution [12]. The effect becomes more pronounced when the maximum aggregate size increases. This is one of the reasons why the size and amount of aggregates are limited in ECC. The aggregate in standard ECC is fine silica sand with a maximum grain size of 250 μm and a mean size of 110 μm. The sand content of ECC is normally less than 30% of the weight of the solid materials. The low volume of sand and thus high volume of cementitious materials in ECC results in large drying shrinkage, an increase in material cost and a decrease in material eco-efficiency.

The adjusted mixing sequence was applied to design a version of HVS-ECC [16]. River sand with the particle size ranging from 0.25 to 0.5 mm was used in ECC. The addition of sand might cause poor particle packing on the surface of fibers and thus a poor fiber–matrix interface. Silica fume was added in order to improve the fraction-based bond of the fiber–matrix interface [17]. Table 3 gives the mix compositions of HVS-ECC. Sand was mixed in S2 and S2A but not in S1. In S2 and S2A, the amount of sand was

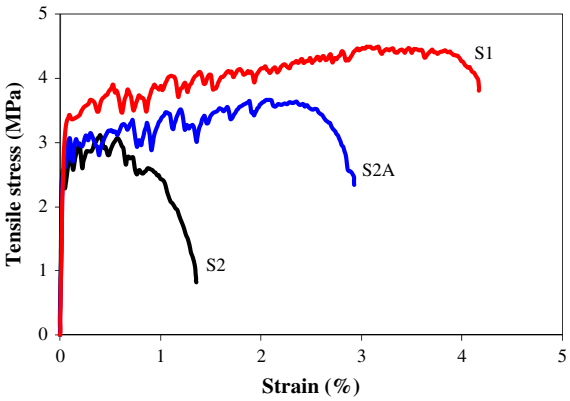

Fig. 12. Typical uniaxial tensile stress–strain curves of ECC and HVS-ECC at the age of 28 days. S1 and S2 were mixed following the standard mixing sequence, and S2A was mixed following the adjusted mixing sequence.

Table 4
Tensile strain capacity and ultimate tensile strength of ECC and HVS-ECC.

Mixture	Tensile strain capacity (%)	Ultimate tensile strength (MPa)
S1	3.7	3.8
S2	0.5	2.9
S2A	2.2	3.5

the same as the total amount of the other solid materials. The fiber content in S1 was 2% by volume and it was 1.2% by volume in S2 and S2A. S1 and S2 were mixed following the standard mixing sequence. S2A was mixed following the adjusted mixing sequence as follows: (1) all solid materials except sand were first mixed with water and superplasticizer at low speed for 1 min and at high speed for 2 min; (2) PVA fibers were added and mixed at high speed for 2 min; (3) sand was then added and mixed at high speed for another 2 min. The casting and curing procedures were the same as described in Section 2.3.

The uniaxial tensile test, as described in Section 2.4, was used to study the tensile behavior of HVS-ECC. The typical uniaxial tensile

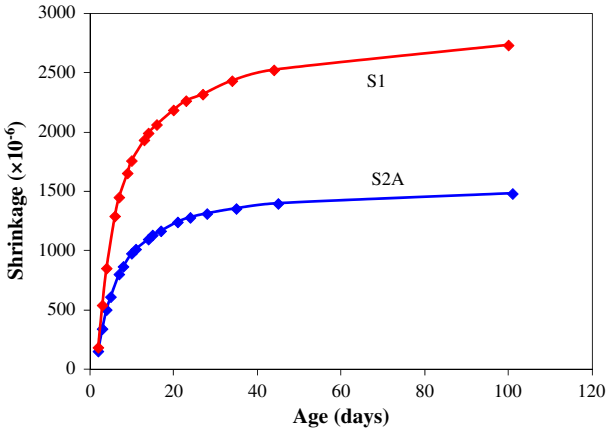

Fig. 13. Drying shrinkage of ECC and HVS-ECC at a temperature of 20 °C and RH of 50%.

stress–strain curves of S1-3 at the age of 28 days are plotted in Fig. 12. The tensile strain capacity and the ultimate tensile strength, calculated by averaging the results of the four measurements, are given in Table 4. For ECCs mixed following the standard mixing sequence, the addition of sand caused 85% decrease in the tensile strain capacity and 26% decrease in the ultimate tensile strength. The adjusted mixing sequence leads to an improvement of the mechanical properties of ECC. S2A shows a tensile strain capacity of 2.2% and ultimate tensile strength of 3.5 MPa, which were 4.1 times the tensile strain capacity and 1.2 times the ultimate tensile strength of S2. The better tensile performance can be attributed to the improved fiber distribution by adjusting the mixing sequence.

S2A also shows advantage in the dimensional stability. The drying shrinkage of HVS-ECC was measured in accordance to the European standard EN 480-3 [18]. The tests were carried out on prism specimens with the dimension of $40 \times 40 \times 160$ mm^3 exposed to a temperature of 20 °C and RH of 50% after 24-h sealed curing. Fig. 13 shows the drying shrinkage of S1 and S2A measured in the first 100 days. Each value represents the average drying shrinkage of three measurements. At the age of 100 days, S1 shows a drying shrinkage of 2730 μstrain, while S2A shows a drying shrinkage of 1480 μstrain. The addition of sand results in 45% decrease in the drying shrinkage.

The adjusted mixing sequence method was successfully applied in the development of HVS-ECC. The adjusted mixing sequence can recover a large part of the loss of tensile strain capacity and ultimate tensile strength due to the addition of sand. Moreover, the high sand content and the low fiber content also reduce the material cost and improve the eco-efficiency of ECC.

6. Conclusions

A new ECC mixing sequence is developed, aimed at improving the fiber distribution in ECC. In this paper, the influence of the different mixing sequences of water is first investigated by comparing the experimental results of the uniaxial tensile test and the fiber distribution analysis. Extending this concept, a new version of HVS-ECC is developed by adjusting the sand mixing sequence. Based on these results, the following conclusions are drawn:

(1) The adjusted mixing sequence results in an increase in the tensile strain capacity and an increase in the ultimate tensile strength of ECC. The increases are more prominent in the mixtures with a higher w/p ratio. The adjusted mixing sequence does not have a significant effect on the properties of ECC matrix, such as first cracking tensile strength.
(2) Compared with the standard mixing sequence, the adjusted mixing sequence improves the fiber distribution in ECC.
(3) A good correlation between the fiber distribution coefficient and the tensile ductility is found. The improved fiber distribution is responsible for the enhanced mechanical properties of hardened ECC.
(4) The adjusted mixing sequence was applied in the development of HVS-ECC. HVS-ECC mixed following the adjusted mixing sequence showed the improved tensile properties and the decreased drying shrinkage. Considering the low cementitious material and fiber contents, the HVS-ECC is expected to have increased material eco-efficiency and reduced material cost, since the PVA fiber dominates the material cost.

Acknowledgements

This research is financially supported by the Delft Clusters and Heijmans Infrastructure B.V. Their support is gratefully acknowledged. We would like to thank BAS B.V. for their help in measuring the particle size distribution of powder materials. V.C. Li would like to acknowledge the US National Science Foundation CI-Team Grant OCI 0636300 for supporting international research collaboration.

References

[1] Li VC. From micromechanics to structural engineering – the design of cementitious composites for civil engineering applications. J Struct Mech Earthquake Eng-JSCE 1993;10(2):37–48.
[2] Weimann MB, Li VC. Hygral behavior of engineered cementitious composite (ECC). Int J Restoration Build Monument 2003;9(5):513–34.
[3] Lepech MD, Li VC. Water permeability of cracked cementitious composites. In: Carpinteri A, editor. Proceedings 11th international conference on fracture; 2005 [paper 4539].
[4] Li VC. Engineered cementitious composites (ECC) – material, structural and durability performance. In: Nawy E, editor. Concrete construction engineering handbook. Boca Raton: CRC Press; 2007 [chapter 24].
[5] Sahmaran M, Li VC, Andrade C. Corrosion resistance performance of steel-reinforced engineered cementitious composite beams. ACI Mater J 2008;105(3):243–50.
[6] Sahmaran M, Li VC. Durability of mechanically loaded engineered cementitious composites under highly alkaline environment. Cem Concr Comp 2008;30(2):72–8.
[7] Michigan Department of Transportation. Bridge decks going jointless: cementitious composites improve durability of link slabs. Construct Technol Res Rec 2005;100:1–4.
[8] Kunieda M, Rokugo K. Recent progress on HPFRCC in Japan. J Adv Concr Techol 2006;4(1):19–33.
[9] Li VC, Leung CKY. Theory of steady state and multiple cracking of random discontinuous fiber reinforced brittle matrix composites. J Eng Mech-ASCE 1992;118(11):2246–64.
[10] Torigoe S, Horikoshi T, Ogawa A, Saito T, Hamada T. Study on evaluation method for PVA fiber distribution in engineered cementitious composite. J Adv Concr Technol 2003;1(3):265–8.
[11] Yang EH, Sahmaran M, Yang Y, Li VC. Rheological control in the production of engineered cementitious composites. ACI Mater J 2009;106(4):357–66.
[12] De Koker D, van Zijl G. Extrusion of engineered cement-based composite material. In: di Prisco M, et al., editors. Proceedings 6th RILEM symposium on FRC; 2004. pp. 1301–10.
[13] Li VC, Wu C, Wang S, Ogawa A, Saito T. Interface tailoring for strain-hardening PVA-ECC. ACI Mater J 2002;99(5):463–72.
[14] Zhou J, Qian S, Guadalupe Sierra Beltran MGM, Ye G, van Breugel K, Li VC. Development of engineered cementitious composites with limestone powder and blast furnace slag. Mater Struct 2010;43(6):803–14.
[15] Kobayashi K. Fiber reinforced concrete. Tokyo: Ohm-Sha; 1981.
[16] Zhou J, Qian S, Ye G, van Breugel K. Engineered cementitious composites with low volume of cementitious materials. In: Oh BH, editor. Proceedings FramCos-7; 2010. p. 1551–6.
[17] Yan H, Sun W, Chen H. Effects of silica fume and steel fiber on the dynamic mechanical performance of high-strength concrete. Cem Concr Res 1999;29(3):423–6.
[18] EN 480-3. Admixtures for concrete, mortar and grout – test methods – part 3: determination of shrinkage and expansion. European Standard; 1991.